RESEARCH ARTICLE

Study of 4A and 5A zeolite as a catalyst material in a catalytic converter for NO emission reduction in a CI engine

Premkumar Subramanian[1] · Balaji Gnanasikamani[1]

Abstract

The major contribution to atmospheric air pollution is from the heavy vehicular emission. At present, it is rising at an alarming rate. These automotive pollutions can be reduced to a great extent by the exhaust gas after-treatment methods. Among these, catalytic converter (CC) is the major source to reduce regulatory emission in the internal combustion (IC) engine. Most catalytic materials work in some specific temperature ranges, and they are also costly. In this study, the zeolite 4A (ZSM 4A) and zeolite 5A (ZSM 5A) powder were converted into a solid mold and tested as a catalytic material in the converter. The experimental readings were taken with the fabricated CC at the exhaust with various loads (0, 4, 8, 12, and 16 kg) in the single-cylinder Kirloskar 5.2 kW diesel engine. Waste plastics were pyrolyzed into oil and blended with diesel in the 50:50 ratio of diesel plastic blend (DPB) for this study. Nitrogen oxide (NO) and hydrocarbon (HC) were reduced by 18% and 22% respectively for ZSM 5A and 12% and 16% respectively for ZSM 4A.

Keywords Diesel engine · Waste plastic oil · ZSM 4A · ZSM 5A · NO emission

Introduction

Globally, more than 60 million vehicles are manufactured on a yearly basis, and 850 million vehicles are under operation (Chen et al. 2017). Automobile production is projected to reach 1400 million by 2030 (Sachuthananthan et al. 2019). Waste plastic recycling is essential in the present scenario. In these wastes, only 60% of the disposed waste plastic material in India is recycled. The non-degradability of plastic wastes is a major concern despite its desirable characteristics, such as being a lightweight material and the possession of resilience. These plastics are analyzed and interpreted extensively in terms of non-degradability and waste management (Raj et al. 2019). The plastic waste can be recycled into fuel as a result of chemical change due to the relevance of the chemical treatment processes involved. The potential of waste plastic oil usage needs to be analyzed

in detail. Biofuel, waste plastic oil, waste tire oil, and other fuels are considered major alternative fuels for compression ignition (CI) engine usage (Pandaa et al. 2016). The plastic conversion into fuel through pyrolysis is extremely important. Also, it is a significant alternative when compared to other sources. The advantage exists in the form of a reduction in the oil-import protection of the environmental sources. The undesirable plastic converts with HC possess elevated calorific value when compared to the other oils (Singha et al. 2019). Researchers have investigated the potential of waste plastic pyrolysis in the formation of plastic oil. They reported that the usage of low-temperature plastic oil resulted in high brake thermal efficiency. Also, the exhaust emissions were low at high temperatures (Dayana et al. 2016; Singh and Ruj 2015). The plastic oil and its blends with diesel combustion, emission characteristics, and performance were investigated. A single-cylinder Kirloskar engine using this waste plastic oil produced the same performance, and brake thermal efficiency was similar to a normal CI engine (Singh et al. 2019; Premkumar and Balaji 2021). But carbon monoxide (CO) emission was increased in waste plastic oil usage compared to diesel (Balaji and Cheralathan 2015; Balaji and Cheralathan 2016; Bagus et al. 2015; Melkon et al. 2006). The liquid plastic fuel possesses a better calorific value when compared to diesel (around 40 MJ/

✉ Balaji Gnanasikamani
  balajig@srmist.edu.in

1 Department of Mechanical Engineering, SRM Institute
   of Science and Technology, Kattankulathur, Tamil Nadu,
   India 603203

Kg). The reduced viscosity of the plastic oil minimizes the nitrogen and sulfur in the exhaust system. Many researchers used the pyrolysis procedure for mixing individual waste plastic variants like polypropene (PP), polyethylene (PE), and polystyrene (PS) with the waste plastic (Nikolajsen et al. 2006; Lai et al. 2003; Zhang et al. 2005).

At temperatures between 500 to 600 °C, the high viscosity oil is produced consisting of long-chain hydrocarbons. This resulted in the formation of wax as an oil-phase product mass which reduced the undesirable emissions. The CC implementation effectively reduces the CO and HC emission in internal combustion (IC) engines (Godwin et al. 2005; Singha et al. 2019). The global pollution due to a large number of vehicles is very high. As a result, new international norms are developed to keep the pollution levels under control. The CC reduces CO and HC emissions using zeolite as a catalyst. The monolith catalyst design was varied, and a suitable design was identified for emission reduction. By varying the cone angle and the diameter of the honeycomb structure, the monolith catalyst was fabricated. The brake thermal efficiency was found to increase by 35% (Miandad et al. 2018; Bharathiraja et al. 2019; Dayana et al. 2016). When the monolith catalytic converter dimensions were kept at 100×50 mm, a decrease in emission was observed. The zeolite was obtained from the fly ash using alkali fusion, followed by hydrothermal treatment. Among the catalysts, the coal fly ash gives the maximum feed conversion to a lighter product.

While considering selective catalytic reduction (SCR) and selective non-catalytic converter (SNCR), ammonia plays a major role. It is responsible for the reduction of NO_x in flue gases. To reduce NO, the coal fly ash as an adsorbing material was suggested. The ammonia gets adsorbed on the coal fly ash surface. The adsorption capacity varies with various parameters such as surface area, pressure, temperature, and unburnt carbon particles. In this process, the zeolite was synthesized using coal fly ash as a catalyst to reduce NO, HC, and CO. Fe-zeolite and Cu-zeolite were found to be more efficient when compared to the commercial zeolite. The speed and load of the engine were varied to obtain the desired results. The in-house zeolite was able to reduce more emissions when compared to the conventional CC (Raganati et al. 2014; Hedin et al. 2013). The combustion of fuel accounts for 81% of the world's industrial energy and remains the dominant supply of energy. Automobiles release nearly two different types of exhaust emissions. Zeolites possess calcium, sodium, and potassium. One of the significant characteristics of zeolite is its ability to be readily dehydrated and rehydrated. They can be used as molecular sieves and powders. Zeolites are micro-porous aluminosilicate minerals, which are generally used as catalysts and commercial adsorbents (Xia and Tang 2012). Zeolite has the property of absorbing impurities. The structure of zeolite is porous, and hence, it has the ability to trap cations. These cations can be exchanged with others in a loosely held contact solution. An example of zeolite is $Na_2Al_2Si_3O_{10}$. These are used as catalysts in several acid-catalytic reactions due to their acidic nature. Natural zeolite is formed when volcanic rocks and ash layers react with alkaline groundwater. Natural zeolites are rarely pure, and they are contaminated with various substances. These naturally occurring zeolites are not used in commercial applications where purity and uniformity are required. The zeolites consist of silicone (Si), oxygen (O_2), aluminum (Al), zinc (Zn), tin (Sn), and titanium (Ti). The term "molecular powder" refers to a particular property of the material reflecting the tendency of selectively sorting molecules based on size. The zeolites possess a regular molecular pore structure. Zeolites are widely used for the specific separation of gases and removal of NO_2, CO_2, SO_2, and H_2O from the exhaust gas. They are also used to separate the noble gases (Zhang et al. 2016).

Zeolites are mostly used as catalysts and/or adsorbent materials. Zeolites have thus proved useful in systems that emit volatile compounds (VOCs), toxic species, stationary deNOx, and automotive exhaust emission treatments. Kim et al. (2004) examined the silicalite material for its hydrophobic characteristics, which enable it to preferentially adsorb HCs over water contained in the automotive exhaust. Various zeolites including H-ZSM-5 (Li et al. 2005), Cu-ZSM-5 (Houeida Issa Hamoud et al. 2019), and SSZ-33 (Elangovan et al. 2004) have also been studied as HC trapping materials for treating DOC. Zeolites ZSM-5 have been found to be beneficial. Zeolites are substantially more stable than VOx/TiO_2 at high temperatures and are active for NH_3-SCR when replaced with the proper charge-balancing cations. Beale et al. (2015) investigated on the effect of Si:Al on the nature of the Cu active sites and also detected lower Si:Al ratios resulting in a wider amount of Cu^+ production at 180 °C using a same gas composition. The zeolite framework, which has significant ion-exchange capacity, excellent thermal stability, a diversity of pore apertures, and relatively high surface areas, frequently affects the internal diffusion of the guest molecules. The majority of heterogeneous reactions that take place over zeolite catalysts rely on the fact that these catalysts' micropores are similar in size to the molecules that are adsorbed.

A two-way CC is also called "oxidizing-catalyst" because it does two simultaneous actions:

1. Reduction of nitrogen oxides to nitrogen (N_2) $2CO + 2NO \rightarrow 2CO_2 + N_2$
2. Oxidation of CO into CO_2: $2CO + O_2 \rightarrow 2CO_2$
3. Oxidation of HC to CO_2 and H_2O: $C x H_2 \times 2 + [(3x+1)/2] O_2 \rightarrow x CO_2 + (x+1) H_2O$

Three-way catalytic converters have the additional advantage of converting nitrous oxide (N_2O) into nitrogen dioxide (NO_2). They work on the principle of oxidation and reduction. Precious metals such as platinum (Pt), palladium (Pd), and rhodium (Rh) are used as catalysts to convert exhaust gases into harmless entities. A three-way catalytic converter has three tasks.

Based on the literature survey honey-comb structure has been used as a wash-coated material to reduce emission in IC engine. Chemicals such as Pd, Pt, Rh, and zeolite are coated in the catalytic converter. But our research was based on the development of a mold for the reduction of emission in IC engine. No literature has been found based on the comparison of zeolites 4A and 5A. Plastic oil was used in IC engine for the purpose of th combustion process and emission reduction in different blends but no one related the plastic oil with the catalytic converter. Due to this research gap, we developed a zeolites 4A and 5A-based mold in the exhaust manifold pipe in IC engine. Accordingly, plastic oil blend was included in the pre-treatment process. Plastic oil blend and catalytic converter are used to reduce and convert harmful emissions such as NO, HC, and CO to harmless H_2O and CO_2.

As previously mentioned, plastic oil is a promising way to increase thermal efficiency and decrease emissions in IC engines by catalytic converter (CC) acting as a catalyst. The primary goal of this study is to determine if CC can adhere to strict NO, HC, and CO emission regulations. However, previous studies mainly focused on the zeolite catalyst not using plastic oil combine with CC. Few researchers mainly focused on plastic oil and blend plastic oil's effect on diesel engine and combustion process but not focused on plastic oil with CC. It is urgently necessary to replicate the different typical aging system conditions to reduce emission. Therefore, the present study investigates the plastic oil and after-treatment techniques used to reduce emission in a diesel engine. Zeolite-based catalysts were compared which is best to reduce emission in IC engine. In past studies, zeolite was used to reduce emission in IC engine not compared to other zeolite 4A and zeolite 5A catalysts which is best to reduce engine exhaust emission in IC engine. The synthesis catalysts were evaluated for their emission and performance. In addition, catalyst characterization was also incorporated with its emission behavior and identified in detail using FTIR, XRD, SEM, and TEM both before and after exhaust gas passes through the catalyst and was analyzed.

Materials and methods

Plastic oil

Waste plastic is converted into useful oil through the pyrolysis process in the absence of oxygen. In the current investigation, the waste plastic, which was collected from different areas and sources, is heated in a temperature range of 250–370 °C for 1 h in a pyrolysis reactor vessel in a step-by-step manner. Due to this, the dioxins are formed as furans. These impure chemical reactants are easily destroyed by the catalytic processes. Consequently, different types of waste plastic blends can be used in the pyrolysis reactor and separated in the condenser using the fractional distillation process resulting in the formation of pure waste plastic oil. Figure 1 shows the plastic oil chemical structure. The properties of the test fuels are given in Table 1. The values of the properties were taken from the various reference papers. The mixing ratio of waste plastic and C_{10}-C_{30} organic compounds was considered. Plastic oil, compared to diesel, has a low calorific value and less sulfur content. The oil-based physical and chemical properties were determined using the American Society of Testing and Materials (ASTM) standards and compared with the 50:50 blend. The properties and chemical formation of the plastic oil, specifically as a DPB, are very similar to neat diesel.

Conversion of plastic oil via pyrolysis method

Plastic oil was purchased from Srinivasa Enterprises India Private Limited, Chennai. The waste plastic oil was converted into pure plastic oil via the pyrolysis process. The plastic oil obtained by the pyrolysis process contains approximately 93% yield, 5% residue, and 2% gases. Temperature range about 32 to 280 °C, and the yield was formed after 3 h duration.

Preparation of activated ZSM 4A and ZSM 5A

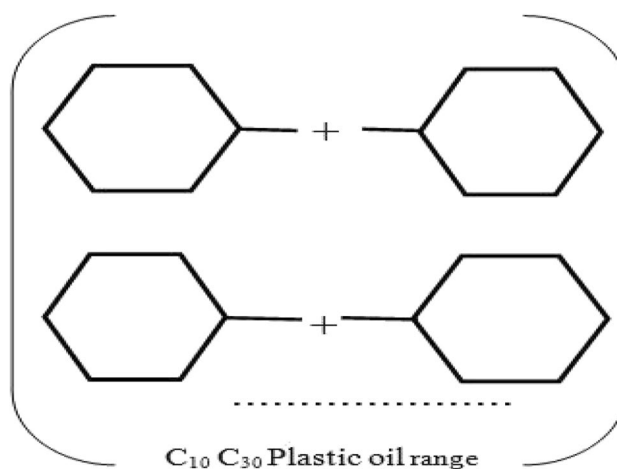Table 2 shows the composition of ZSM 4A and ZSM 5A. The zeolite 4A powder (40%) has the components of

Fig. 1 Structure of plastic oil. *Courtersy Hao Tang et al. (2012)

Table 1 Properties of test fuels

Properties	Test standard	Diesel	Waste plastic oil	Diesel plastic blend (DPB)
Calorific value (kJ/kg)	ASTM D240	44,450	42,350	43,540
Flash point (°C)	ASTM D93	51	43	47
Fire point (°C)	ASTM D93	57	64	59
Pour point (°C)	ASTM D97	7	< −14	-
Ash content (%)	ASTM D482	0.14	0.0035	0.045
Sulphur content (% wt.)	ASTM D 129	<0.035	<0.002	<0.015
Colour		Orange	Pale black	Pale black
Kinematic viscosity (Cst) at 40 °C	ASTM D 445	2.11	2.51	2.31
Aromatic content (%)	ASTM D5186	20	55	34
Density (kg/m^3)	IP 131/57	834	792	798
Cetane number	ASTM D613	55	51	52
Gum in existent (gm/m^3 max.)	ASTM D 381	36	-	-
Specific gravity at 30 °C	ASTM D891	0.87	0.82	0.85
Carbon residue (% of wt)	ASTM D189	0.7	0.5	0.6
Specific heat (kJ/kg K)	ASTM E1269	2.2	48	-

*Courtesy – Balaji Gnanasikamani et al. (2015), Mani et al. (2009)

Table 2 Composition of ZSM 4A and ZSM 5A

Components	ZSM 4A	ZSM 5A
SiO$_2$	33.10	33.20
Al$_2$O$_3$	27.50	28.01
Fe$_2$O$_3$	0.36	0.32
TiO$_2$	0.16	0.15
Na$_2$O	20.01	15.90
K$_2$O	<0.1	<0.09
Loss of ignition	18.34	17.89

bentonite clay (10%), plasticizer (10%), white cement as a binder (10%), and distilled water (30%). These components are stirred for 2 h resulting in the form of a zeolite paste, as shown in Fig. 2. Holes of 2 mm diameter are drilled in the mold cavity. The finishing of the plastic pipe is covered by the molding material. The combination was sustained at atmosphere temperature for 24 h. After this, the plastic cover was removed, and the final mold was heated in a muffle furnace from 150 to 450 ℃. A time interval of 20 min was followed for a step-by-step increase in temperature till the substance attains sufficient hardness.

The ZSM 5A powder (53%) was mixed with bentonite clay (8%), carboxymethyl cellulose binder (5%), and distilled water (34%). The components were stirred constantly to form a paste. The applied torque was monitored during stirring to ensure consistency for homogeneous mixing. The zeolite paste was placed in the prepared mold cavity, and uniform pressure was applied to ensure an absence of gaps, as shown in Fig. 3. The hole pattern was created on the mold uniformly (10 mm) with the help of plastic pipes. The

prepared mold was dried for 96 h in direct sunlight. After drying, the pipes were removed from the mold. The resulting mold was kept in the furnace initially at 100 °C with an increase of 50 °C every 30 min until the temperature reaches 450 °C with a soaking period of 1 h. Then, it is finally kept for 1 h for the removal of calcination.

The ZSM 4A and ZSM 5A were calcinated in an air atmosphere for 4 h at 500 °C. The main purpose of activating the catalyst is to reduce the emission drastically in the IC engine. According to the chemical process hypothesis, the chemical reaction phase should be included because it is where many intricate chain reactions take place. These reactions are found to reduce emissions. In this investigation, the catalytic converters are used to reduce pollutants in spite of their reactions at low temperatures and to function under optimal circumstances. The reaction mechanisms are revealed in Figs. 4 and 5 (Madasamy et al. 2012).

Fabrication of casting

The outer casing of the CC was made using hollow steel tubes. The tubes were welded together to prepare the outer case. The main CC casing section was fabricated with a diameter of 8 cm and a length of 60 cm. Four uniform holes were drilled with 8 mm diameter as shown in Fig. 6. Tungsten inert gas welding (TIG) was used to ensure proper welding between different parts of the CC. To enhance the serviceability of the casing, external threads were cut on one side of the main section, and internal threads were cut on the reducer. To ensure proper fitting, the threads were cut up to a length of 2 cm.

Fig. 2 Photographic view of zeolite mold 4A
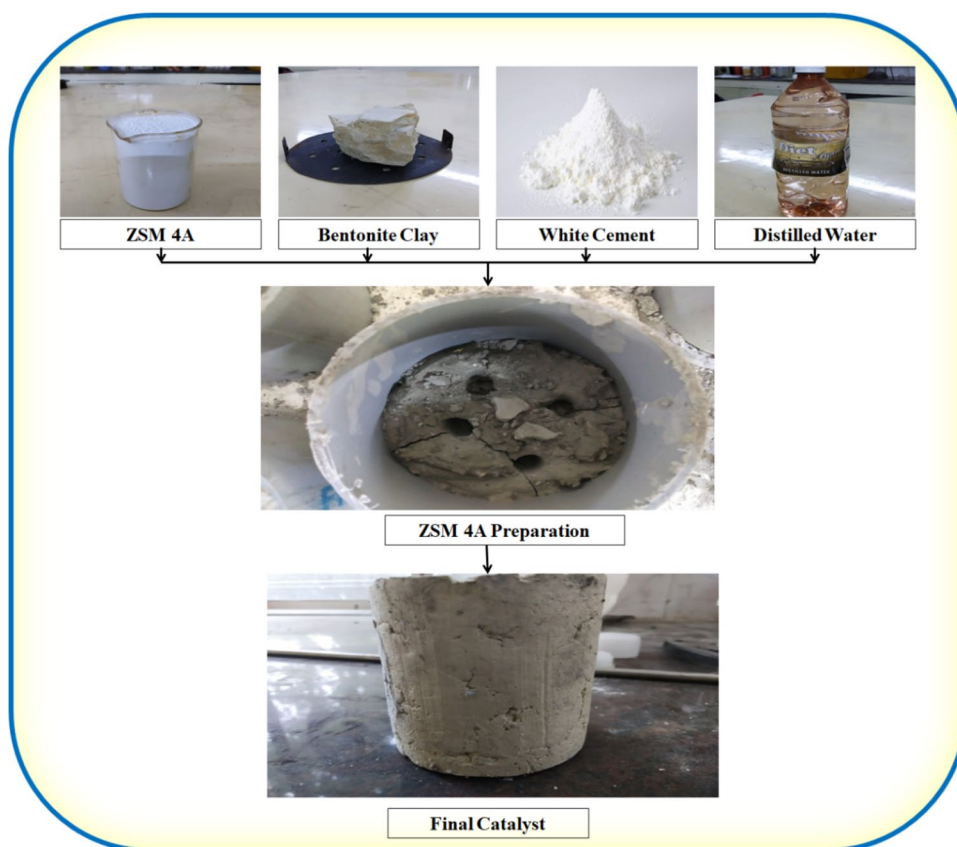
Experimentation

The experimental work was done using a Kirloskar make 5.2 kW, water-cooled DI engine connected to an eddy current dynamometer, with natural aspiration. An AVL gas analyzer was used to measure the exhaust gas in the tailpipe. The smoke meter was also used to measure the % of smoke opacity. Figures 7 and 8 represent the layout and photographic view for the experimental setup.

Results and discussion

Characterization

ZSM 4A and ZSM 5A catalyst samples were subjected to XRD characterization. These catalysts have strong diffraction pattern with numerous features. The XRD patterns of the ZSM 4A and ZSM 5A catalysts before and after the investigations were given in Figs. 9, 10, 11, and 12. There are adsorption distinctions between the ZSM 4A and ZSM 5A catalysts due to the phase transformation between the catalysts. For ZSM 4A, sharp peaks were seen at 2θ values of 7°, 10.2°, 12.6°, 16.3°, 21.8°, 24°, 26.4°, 27.2°, 30.6°, 31°, 31.1°, 32.7°, 33.6° and 34.1° that has been reported in the literature (Zamani et al. 2013) which can be indexed to the

(200), (220), (222), (420), (440), (600), (622), (640), (642), (694), (600), (840), (842), and (664) reflections of the cubic crystalline system for before and after the investigation. Additional peaks in the powder diffraction pattern would indicate the presence of a crystalline impurity. The XRD spectrum of the zeolite 5A is presented in Fig. 11. Zeolites are known to give diffraction peaks at 2θ = 9.05°, 15.71°, 23.36°, 24.18°, 25.61°, and 30.17° attributed to (111), (051), (313), (323), and (062) planes, which is a pentasil structure of ZSM-5A zeolite equivalent to the JCPDS card no. 89–1421 (Jesudoss et al. 2017). The presence of the aforementioned peaks in zeolite is indicative of the successful formation of ZSM 5A. We have also calculated the mean crystalline size of the samples using the Debye–Scherer equation. The average crystalline of the samples ZSM-5A zeolite was 19.34 nm, respectively. The broadening of the diffraction lines indicates the presence of nanometer-sized crystals. These samples exhibit good crystallinity, and it has the property of observing oxygen from the harmful gases; it observes oxygen from NO and splits it into N_2 and O_2, and HC and CO are converted into H_2O and CO_2.

The FTIR spectra of zeolite 4A before and after treatment are shown in Figs. 13 and 14. In the FTIR spectrum of the zeolite 4A, the characteristic bands for zeolite framework at 566 cm^{-1} due to the external vibration of double four-rings, (Si, Al)-O asymmetric stretching, The board band at around
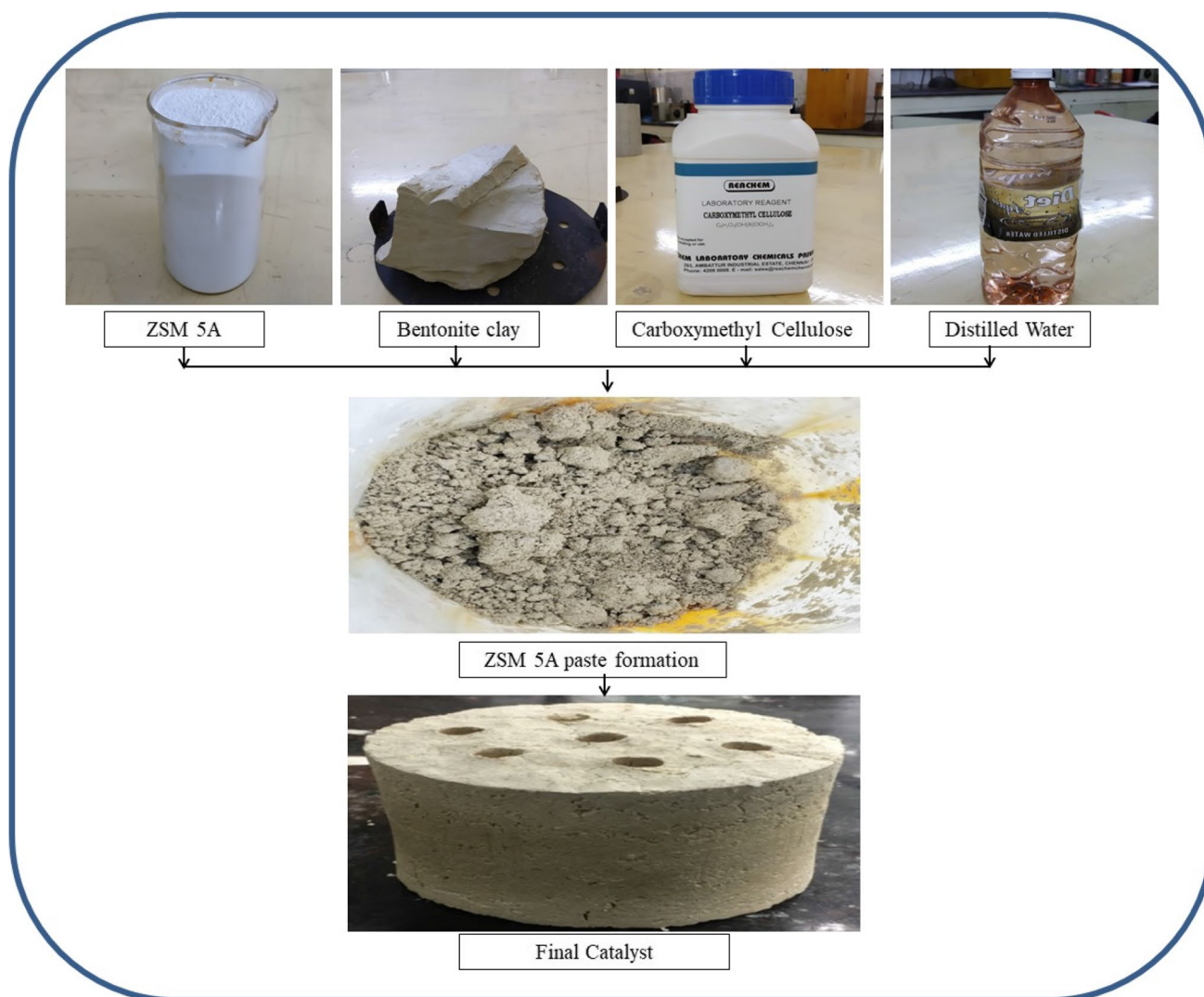
Fig. 3 Photographic view of zeolite mold 5A

3100–3600 cm^{-1} are related to OH. Meanwhile, the FTIR result shows that the major peaks are at 3288 cm^{-1} for –OH, 1735 cm^{-1} for C=O stretching, 834 cm^{-1}, and 547 cm^{-1} (symmetrical stretching vibration of Si–O and Al-O bond of zeolite) (Prasad et al. 2011; Zhao et al. 2009). Due to the availability of hydroxyl groups, hydrogen-bond interaction is possible between the zeolite and the carboxyl group of carboxyl methyl cellulose (CMC). This chemical interaction is reflected in the FTIR spectra (Fig. 13). A major redshift of the main zeolite peak (3288 cm^{-1}) is considered a strong indication for zeolite (Chen and Pan 2021). The zeolite 5A framework vibrations and silanol groups were (as shown in Fig. 15) ~ 1100 cm^{-1} (internal asymmetric stretch), 798 cm^{-1} (external symmetric stretch), and 459 cm^{-1} (T-O bend) corresponding to siliceous materials. The ZSM-5A zeolites display the characteristic bands at 3474 cm^{-1} due to framework Al–OH. The characteristic band of the double five rings of the zeolites is located at 549 cm^{-1} (Chu et al. 2009), which can be used to determine the crystalline degree of the samples (Larsen 2007). The high intensity of the 549 cm^{-1} band suggests that the ZSM 5A has a great crystalline degree, as confirmed by the XRD patterns. The characteristic band of silanol groups is observed at 972 cm^{-1} (Fang and Hu 2006). It is noted that the intensity of silanol groups in the ZSM 5A may be related to the surface areas of zeolites (Fig. 16).

SEM and EDX images of ZSM 4A and ZSM 5A are given in Figs. 17, 18, 19, and 20. ZSM 5A has greater adsorption due to its large particle size with a high degree compared to ZSM 4A. These particles are surrounded in correlation to noble metals as described and also contain higher activity. When compared to ZSM 4A, these intergranular pore structures were more closely packed and easily adsorbed the same shape and size emitted. The size of ZSM 4A before is 4 μm at 20,000 magnifications and
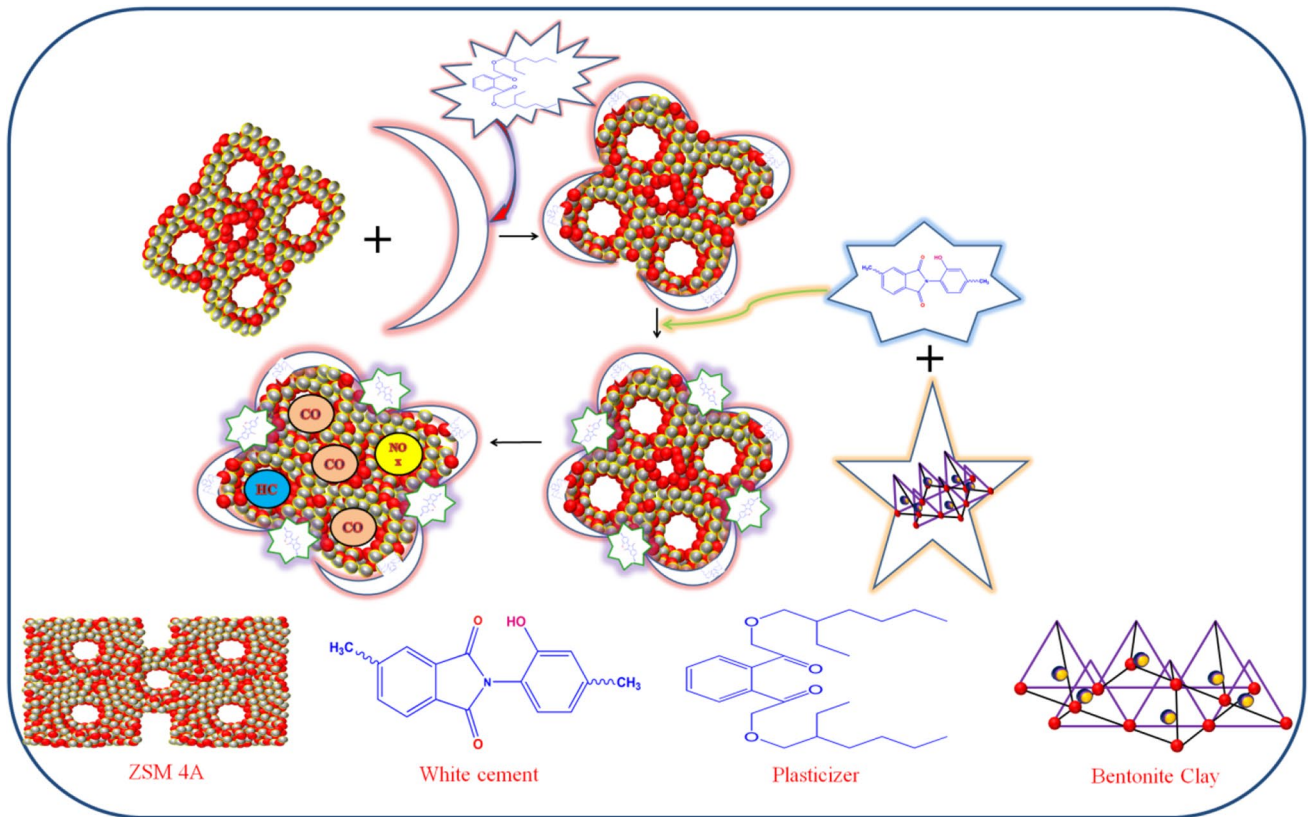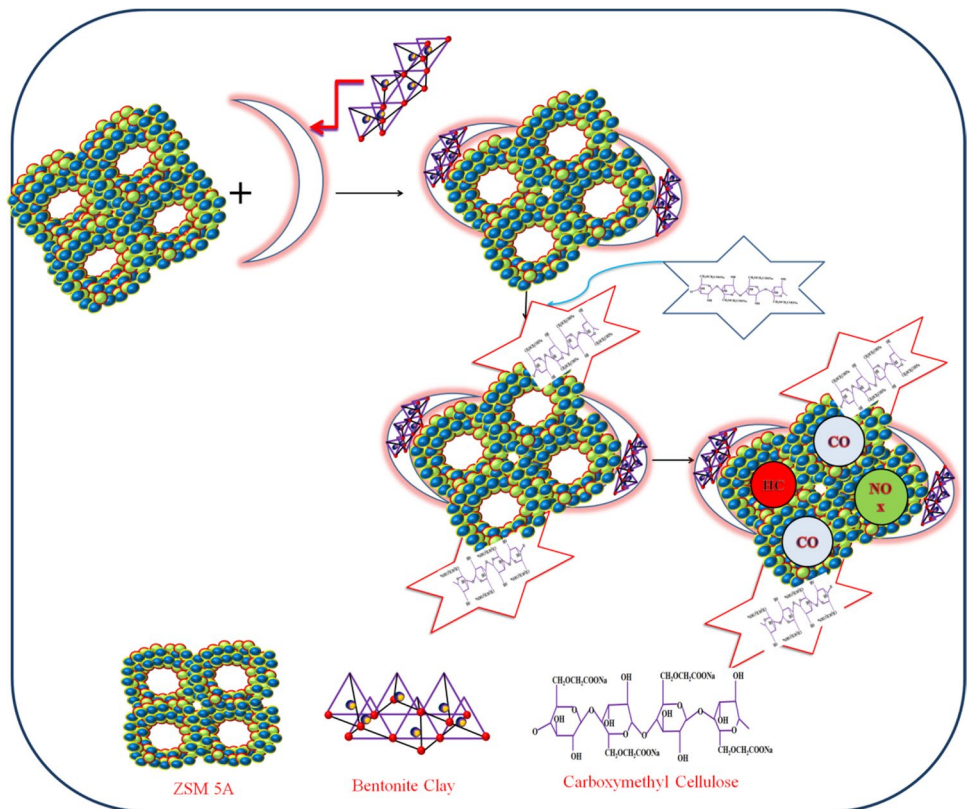
Fig. 4 Detailed chemical reaction pathway of ZSM 4A

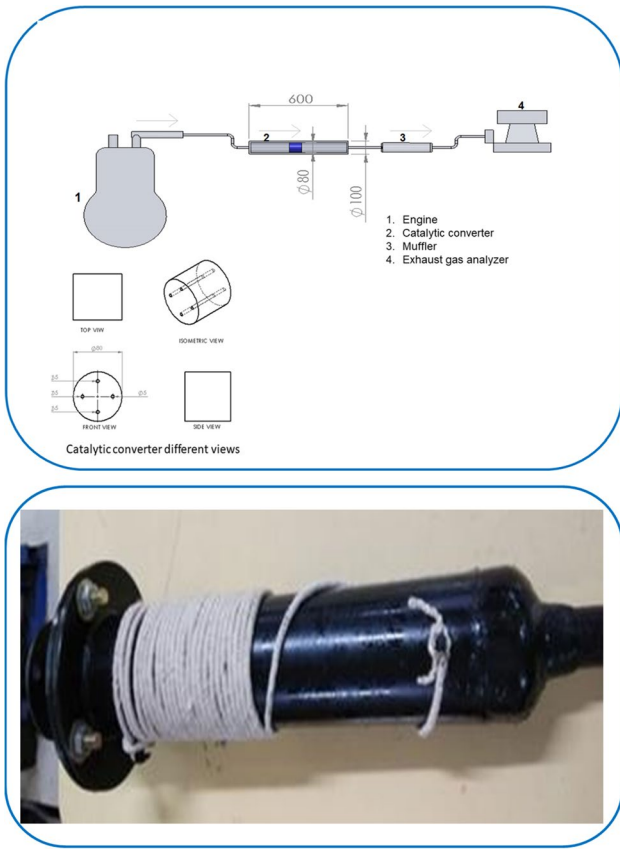**Fig. 5** Detailed chemical reaction pathway of ZSM 5A

Fig. 6 Layout and photographic view of catalytic converter casing

after is 500 µm at 100,000 magnifications. The morphology structure was identified as a cube. As bentonite clay is used as an inorganic binder, the cube structure is formed and visible through the SEM image (Ojuva et al. 2015). The size of ZSM 5A before is 500 µm at 1,000,000 magnifications and after is 500 µm at 100,000 magnifications. The main reason for incomplete elimination is indeed the existence of organic templates from the structure in the zeolite (Follmann and Ernst 2016). This tends to result in mesoporosity and cavity distribution as zeolite is confirmed by nitrogen oxide adsorption analysis.

Emissions characteristics

NO emission During the combustion of the air–fuel mixture, differing types of NO emission were formed, including thermal NOx, fuel NOx, and prompt NOx. The NOx emissions were highly anticipated, which were responsible for various complications. These emissions were reduced using different techniques, but they were not sufficient for the control of NO emissions in the IC engine. These emissions prove to be the most detrimental pollution variants in the ignition stage. The main reasons for this are identified in the combustion process. The components involved in the reactions, the concentrations, the increase in the combustion chamber temperature, and the increased time duration of the combustion process influence the NO formation (Deshwar et al. 2023). Figure 21 shows the emission of NO with an increase in load under DPB usage. During the

Fig. 7 Layout of experimental setup
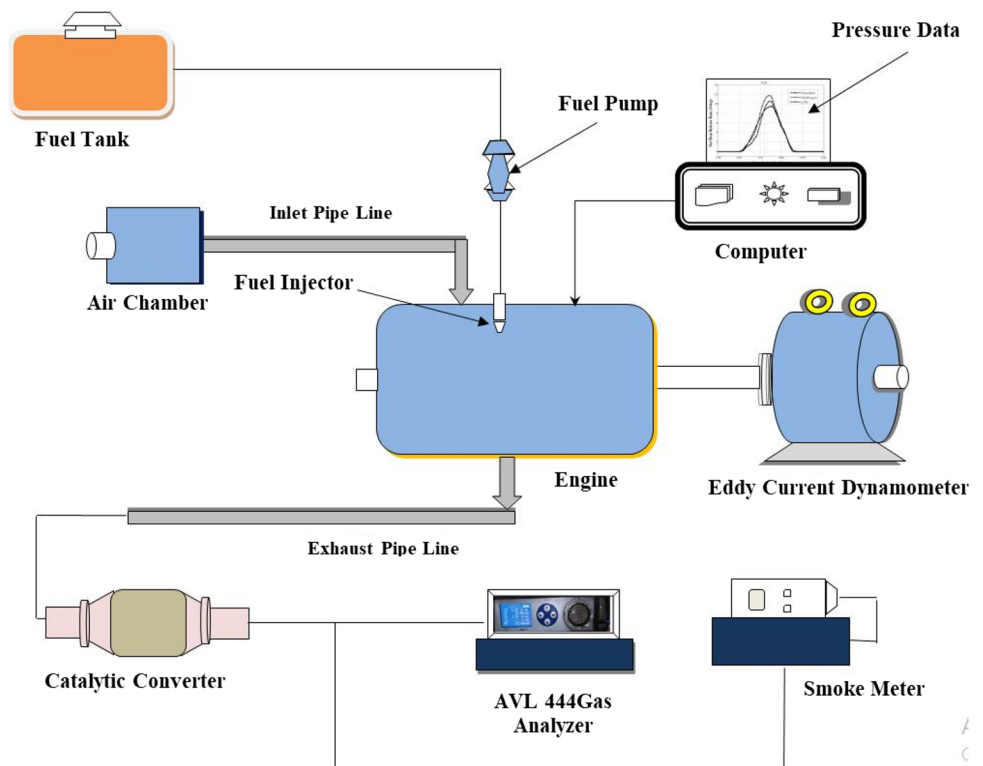
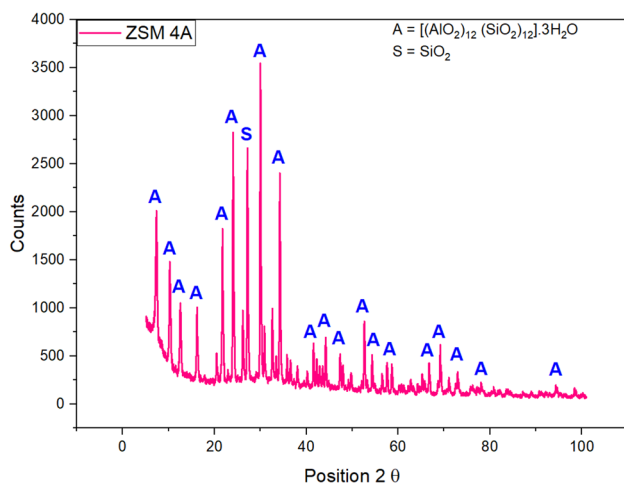Fig. 8 Photographic view of a test engine

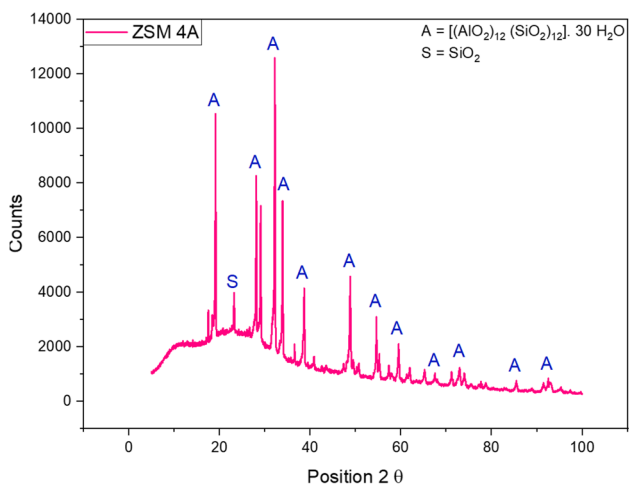Fig. 9 XRD pattern of ZSM 4A before catalyst

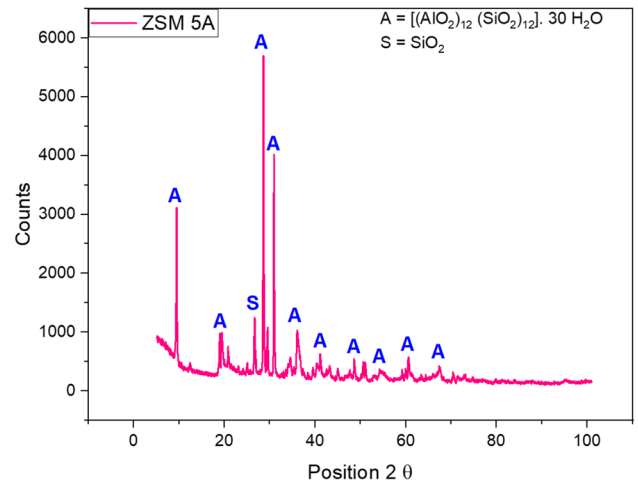

Fig. 10 XRD pattern of ZSM 4A after catalyst

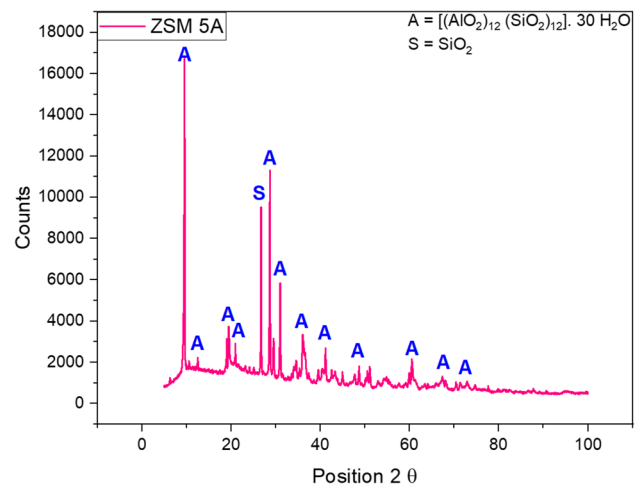Fig. 11 XRD pattern of ZSM 5A before catalyst

Fig. 12 XRD pattern of ZSM 5A after catalyst

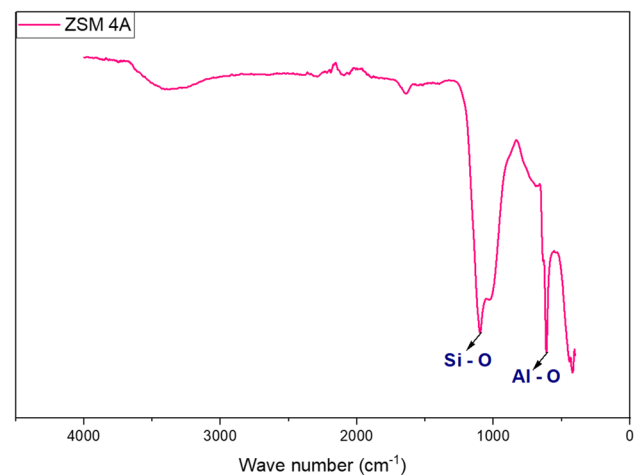Fig. 13 FTIR pattern of ZSM-4A catalyst before

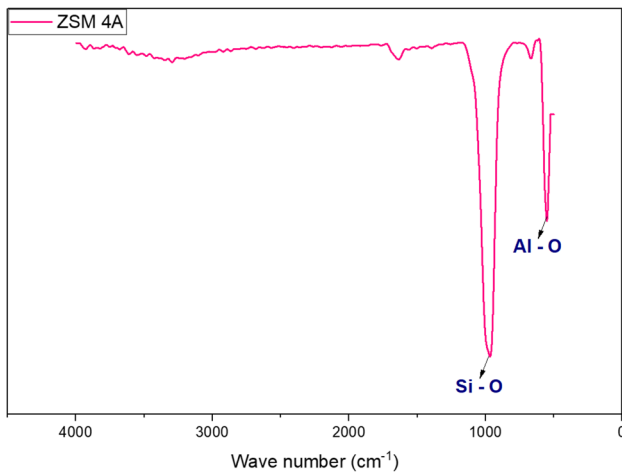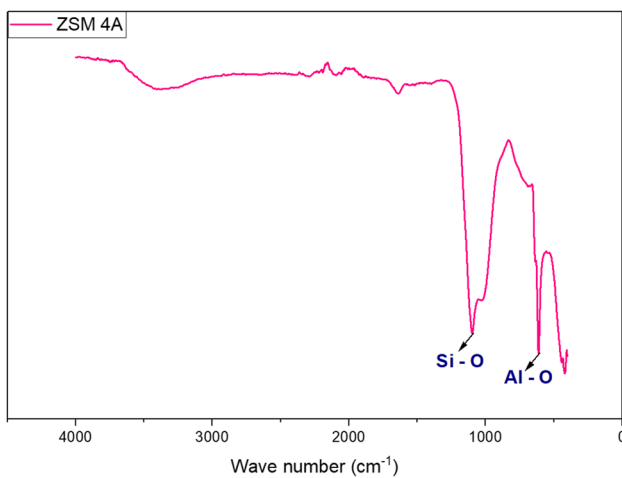**Fig. 14** FTIR pattern of ZSM-4A catalyst after
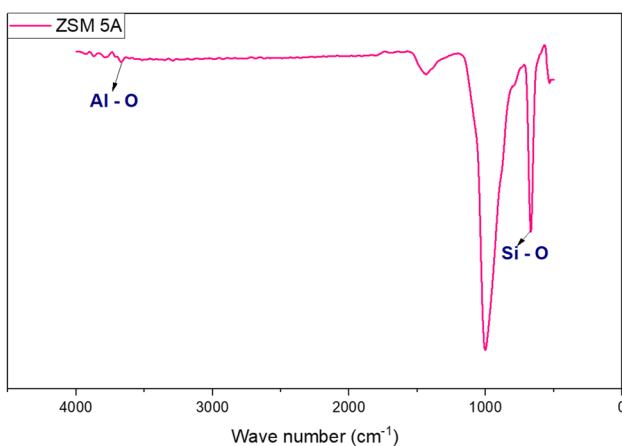

Fig. 15 FTIR pattern of ZSM-5A catalyst before

Fig. 16 FTIR pattern of ZSM-5A catalyst after

combustion of fuel and air mixture in the cylinder, the oxidation of nitrogen results in the formation of NO and NO_2 (Balaji Subramanian 2021). The NO_2 is the main undesirable emission particulate in the CI engine elevated heat release rates (Mani et al. 2009).

The DPB is a higher aromatic content fuel with a significant ring structure. Usually, fuels with ring structures have a high adiabatic flame temperature, which results in a higher heat release rate. The results revealed that the increase in engine load was proportional to the NO emission. Here also, the results show the increase of NO emission with the engine load. Furthermore, the inclusion of the CC resulted in a decrease in NO emission when compared with the DPB. From Fig. 21, it is clear that the NO emission for diesel, DPB, DPB + ZSM 4A, and DPB + ZSM 5A was 1200, 1050, 970, and 890 ppm, respectively. The fuel consumption increases with load to augment the power output and speed, which enhances the cylinder temperature. The NO emission decreases by 12 and 18% for DPB + ZSM 4A and DPB + ZSM 5A compared to DPB.

The emission of the unburned HC is responsible for the smog formation. Incomplete fuel combustion, lower in-cylinder temperatures, and excessive lean mixture formation are the main reasons for HC emission (Mathanraj Vijayaragavan 2021). Other reasons include the fuel viscosity, volatility, and the presence of lesser temperature zones inside the combustion chamber. Higher viscosity results in the formation of huge droplets, and the vapor pressure results in incomplete combustion, which increases the HC emission. Figure 22 shows the variation of HC emission with brake power. For DPB + ZSM 4A, the HC decreased by 16%, and the decrease was 22% under DPB + ZSM 5A usage compared to DPB. The emission was further reduced by passing the exhaust gases through the CC. The reduction was due to the reaction of the exhaust gases with the catalyst.

Figure 23 depicts the variation of CO emission with brake power. The CO emission is particularly harmful as a toxic gas, and it manifests itself primarily as a poor combustion by-product due to insufficient oxygen supply. Another reason is due to the lower rich mixture and flame temperature. This emission reduces under DPB as oxygen levels rise, resulting in better combustion due to the conversion of CO into CO_2 (Toops et al. 2010; Khoramzadeh et al. 2019). Another reason is that the ZSM 4A is an adsorbent by nature. The CC was found to effectively reduce CO emissions. There are also polarized degrees and containment of quadrupole moments in the emission reduction (Battaglia et al. 1981). The comparative features between the ZSM 5A and ZSM

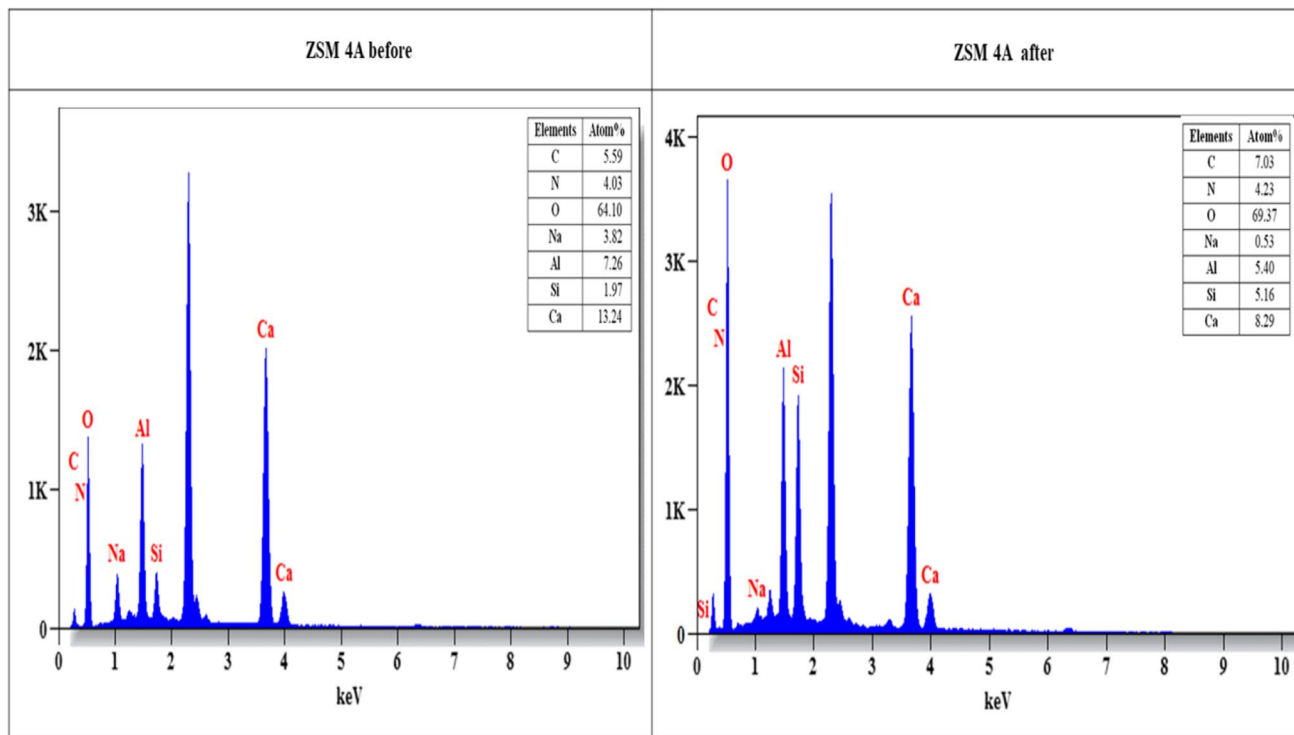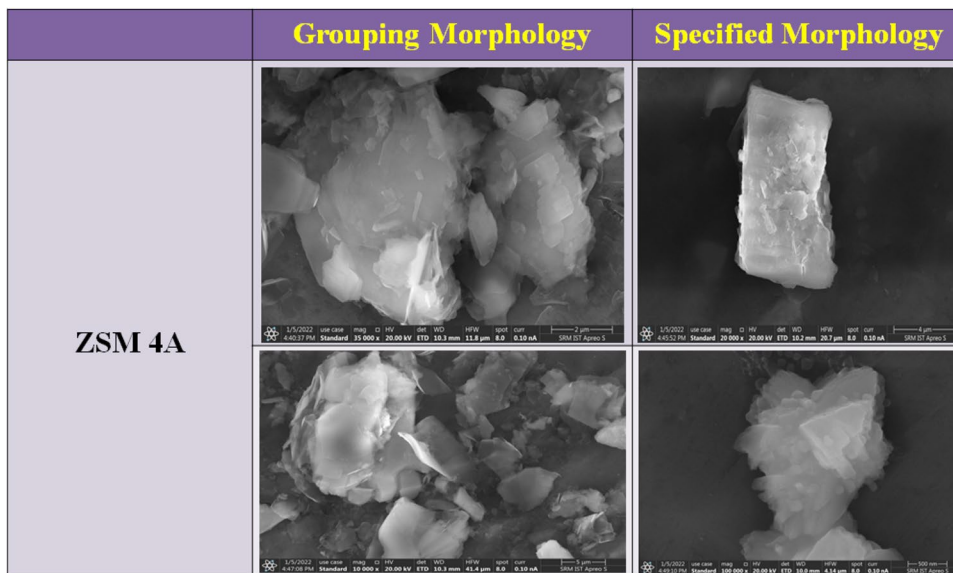**Fig. 17** SEM Image of ZSM-4A catalyst both before and after

Fig. 18 EDX Image of ZSM-4A catalyst both before and after

4A justify the efficiency of the CC to reduce CO emissions. The CO emissions were reduced by 20% when DPB + ZSM 4A were used with the DPB and by 25% when the DPB + ZSM5A were used with the DPB.

Figure 24 shows the variation in smoke emission. The smoke emission for diesel, DPB, DPB + ZSM 4A, and DPB + ZSM 5A were 89, 90, 94, and 98%, respectively. The smoke intensity increases with an increase in engine load, which was observed in all the tests conducted.

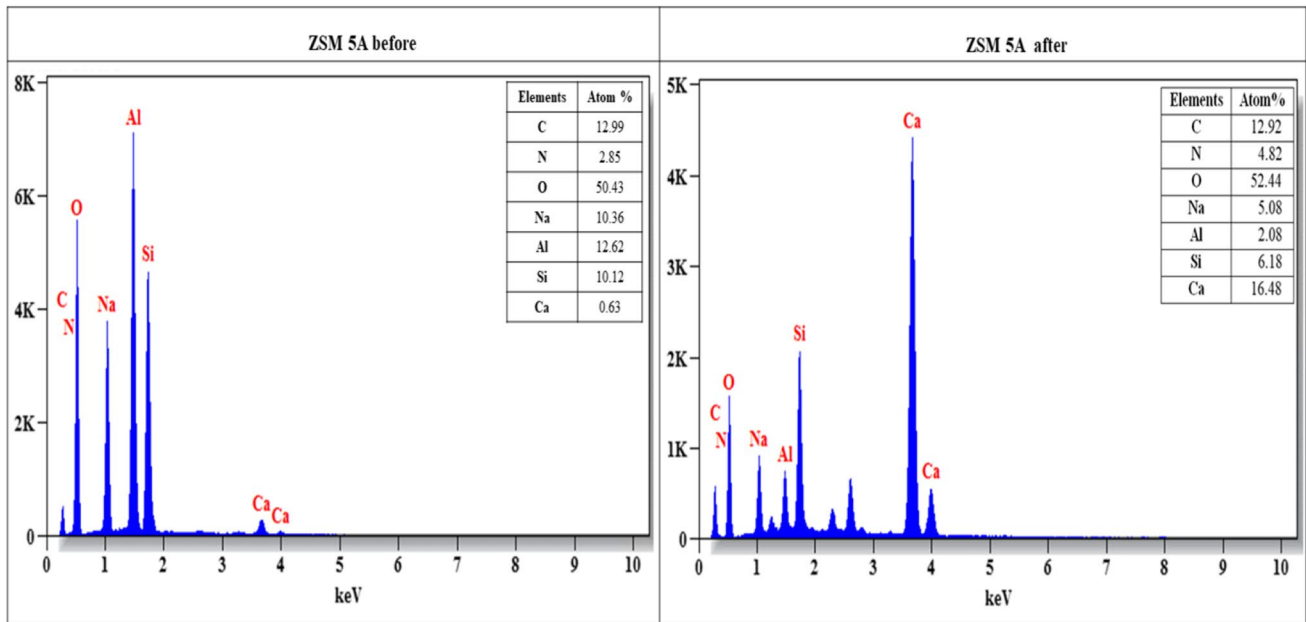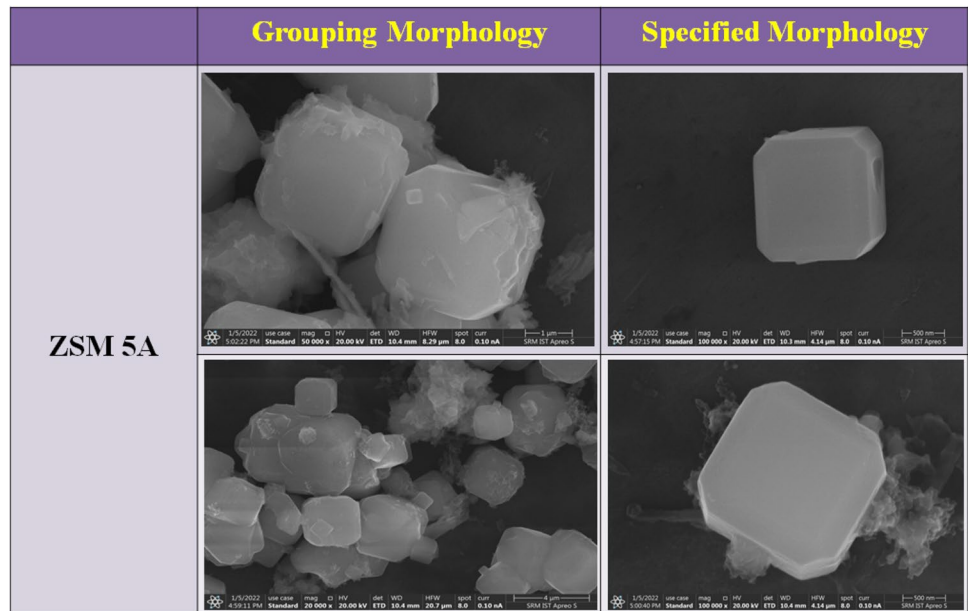**Fig. 19** SEM Image of ZSM-5A catalyst both before and after

Fig. 20 EDX Image of ZSM-5A catalyst both before and after

The smoke opacity decreases by 7% and 12% under DPB + ZSM 4A and DPB + ZSM 5A, respectively, when compared to DPB. The oxygen levels decreased, and the C–C bond levels increased, which resulted in an aromatic content elevation. So, the smoke level was reduced under the DPB + ZSM 5A catalyst usage.

Performance characteristics

The brake thermal efficiency (BTE) was observed under various load changes. The BTE values which are observed under diesel usage were higher when compared to the plastic oil usage. Also, the calorific values and other flow characteristics were low due to the higher viscosity of fuel and the substandard air–fuel mixtures. These factors were responsible for the decrease in the BTE under plastic oil usage compared to
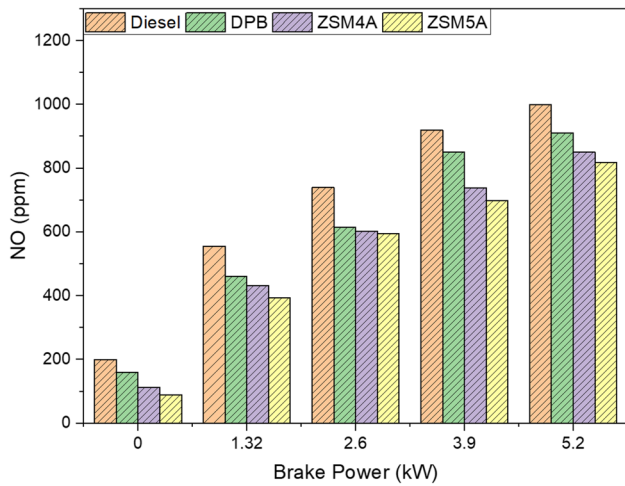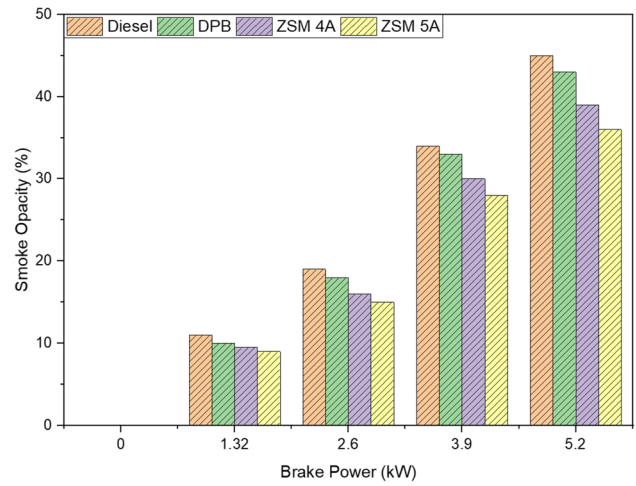
Fig. 21 Variation of NO emission
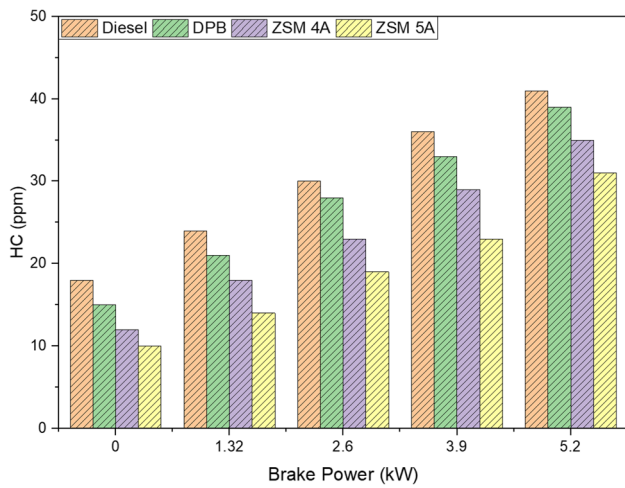

Fig. 22 Variation of HC emission
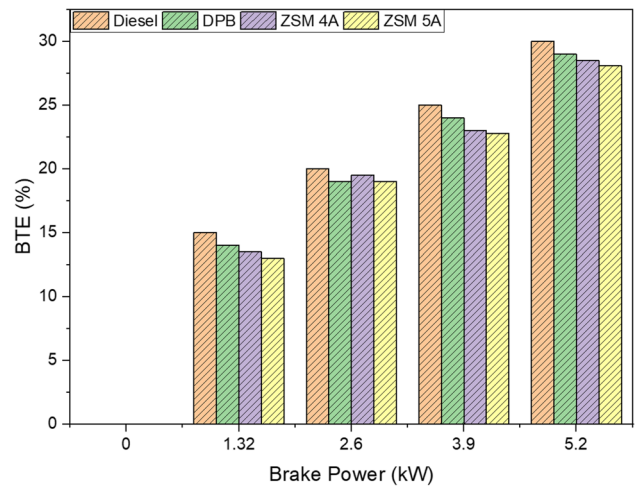

Fig. 23 Variation of CO emission
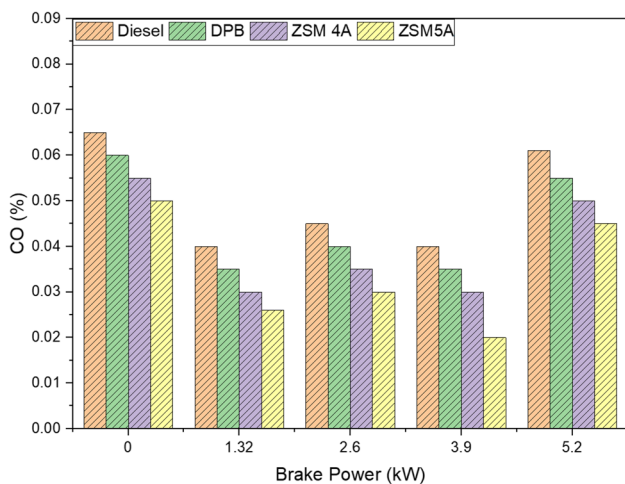

Fig. 24 Variation of Smoke emission

Fig. 25 Variation of BTE

diesel, as shown in Fig. 25. A decrease in BTE, which was noted for DPB + ZSM 5A, was also seen for plastic oil.

Conclusion

The performance and emission characteristics of the DPB fuel in an unchanged CI engine with a CC using ZSM 4A and ZSM 5A catalyst were analyzed experimentally. Based on the results, it was concluded that the adsorption level of the zeolite was augmented at elevated temperatures of the exhaust gas. The catalyst ZSM 5A performed well, resulting in an amplification of the pore structure when compared with ZSM 4A. The other conclusions are as follows:

1. The DPB + ZSM 4A reduced NO emission by 12%, and the DPB + ZSM 5A reduced NO emission by 18% compared to DPB. The ZSM 5A was more effective than ZSM 4A in the reduction of NO emission.

2. The DPB + ZSM 4A and DPB + ZSM 5A minimized the HC emission by 16% and 22% compared to DPB. This was due to the tendency of the DPB + ZSM 5A catalyst to provide oxygen which added the surface lattice oxygen to the HC compounds.

3. The DPB + ZSM 4A and DPB + ZSM 5A minimized the CO emission by 8% and 10%, respectively, compared to DPB.

4. The DPB + ZSM 4A and DPB + ZSM5A decreased the smoke emission by 7% and 11%, respectively, when compared to DPB. There was no significant change in the brake thermal efficiency.

Declarations

Ethics approval and consent to participate Not applicable.

Consent for publication Informed consent was obtained from all individual participants included in the study.

Competing interests The authors declare no competing interests.

References

Achyut Pandaa K, Muruganb S and Singh RK (2016) Performance and emission characteristics of diesel fuel produced from waste plastic oil obtained by catalytic pyrolysis of waste polypropylene, Energy Sources. Part A: Recovery, Utilization, And Environmental Effects, 38. https://doi.org/10.1080/15567036.2013.800924

Bagus Irawan RM, Purwanto P, Hadiyanto H (2015) Optimum design of manganese-coated copper catalytic converter to reduce carbon monoxide emissions on gasoline motor procedia environmental sciences, 23: 86 – 92. https://doi.org/10.1016/j.proenv.2015.01.013

Balaji G, Cheralathan M (2015) Experimental reduction of NOx and HC emissions in a CI engine fuelled with methyl ester of neem oil using p-phenylenediamine antioxidant. J Sci Ind Res 73:177–180. https://doi.org/10.1080/15567036.2012.749314

Balaji G, Cheralathan M (2016) The effect of antioxidant additives with methyl ester of neem oil on the oxidation. Stability. Energy Sources Part a: Recovery, Utilization Environ Effects 38:2454–2461. https://doi.org/10.1080/15567036.2015.1089339

Battaglia MR, Buckingham AD, Neumark D, Pierens RK, Williams JH (1981) The quadrupole moments of carbon dioxide and carbon disulphide. Mol Phys 43(5):1015–1020. https://doi.org/10.1080/00268978100101831

Beale AM, Gao F, Lezcano-Gonzalez I, Peden CH, Szanyi J (2015) Recent advances in automotive catalysis for NOx emission control by small-pore microporous materials. Chem Soc Rev 44:7371–7405. https://doi.org/10.1039/C5CS00108K

Bharathiraja M, Venkatachalam R, Senthilmurugan V (2019) Performance, emission, energy and exergy analyses of gasoline fumigated DI diesel engine. J Ther Anal Calorimetry 136:281–293. https://doi.org/10.1007/s10973-018-7933-0

Chen SJ, Zhu M, Huang YX, Tao ZC (2017) Using 13X, LiX, and Li Pd Ag X zeolites for CO2 capture from post-combustion flue gas. J Appl Energy 191:87–98. https://doi.org/10.1016/j.apenergy.2017.01.031

Chen, Z and Pan K (2021) Enhanced removal of Cr (VI) via in-situ synergistic reduction and fixation by polypyrrole/sugarcane bagasse composites. Chemosphere, 272:129606. https://doi.org/10.1016/j.chemosphere.021.129606

Chu N, Yang J, Li C, Cui J, Zhao Q, Yin X, Lu J, Wang J (2009) An unusual hierarchical ZSM-5 microsphere with good catalytic performance in methane dehydroaromatization. Microporous Mesoporous Mater 118:169–175. https://doi.org/10.1016/j.micromeso.2008.08.048

Dayana S, Sharuddin A, Abnisa F, Mohd W, Wan A (2016) A review on pyrolysis of plastic waste. J Energy Convers Manage 115:308–326. https://doi.org/10.1016/j.enconman.2016.02.037

Deshwar, Pranay, Gaurav Kumar, Balaji Subramanian, Shreyash Hemant Panchal, Venugopal Thangavel, Saleel Ismail, and M. Feroskhan (2023) Simultaneous reduction of NOx and smoke emissions in gasoline-ethanol blended RCCI Engine with biogas as a ternary fuel. Int J Energy Clean Environ 24:2. https://doi.org/10.1615/InterJEnerCleanEnv.2022040767

Elangovan SP, Ogura M, Davis ME, Okubo T (2004) SSZ-33: A promising material for use as a hydrocarbon trap. J Phys Chem B 108:13059–13061. https://doi.org/10.1021/jp047394r

Fang Y, Hu H (2006) An ordered mesoporous aluminosilicate with completely crystalline zeolite wall structure. J Am Chem Soc 128(33):10636–10637. https://doi.org/10.1021/ja061182l

Fedeyko JM, Chen B, Chen H-Y (2010) Mechanistic study of the low temperature activity of transition metal exchanged zeolite SCR catalysts. Catal Today 151:231–236. https://doi.org/10.1016/j.cattod.2009.12.015

Follmann S, Ernst S (2016) Influence of the pore architecture on the selective conversion of ethene to propene and butenes over medium pore zeolites. New J Chem 40:4414–4419. https://doi.org/10.1039/C5NJ03668B

Godwin TP, Mabande SG, Lai Z, Schwieger W, Tsapatsis M (2005) Preparation of b- oriented MFI films on porous stainless steel substrates. Ind Eng Chem Res 44:9086–9095. https://doi.org/10.1021/ie050668s

Hamoud HI, Valtchev V, Daturi M (2019) Selective catalytic reduction of NOx over Cu-and Fe-exchanged zeolites and their mechanical mixture. Appl Catal B 250:419–428. https://doi.org/10.1016/j.apcatb.2019.02.022

Hedin N, Andersson L, Bergstrom L, Yan JY (2013) Adsorbents for the post-combustion capture of CO2 using rapid temperature swing or vacuum swing adsorption. Appl Energy 104:418–433. https://doi.org/10.1016/j.apenergy.2012.11.034

Jesudoss SK, Vijaya JJ, Kaviyarasu K, Kennedy LJ, Ramalingam RJ, Al-Lohedan HA (2018) Retracted article: anti-cancer activity of hierarchical ZSM-5 zeolites synthesized from rice-based waste materials. RSC Adv 8:481–490. https://doi.org/10.5012/bkcs.2013.34.8.2367

Khoramzadeh E, Mofarahi M, Lee C-H (2019) Equilibrium adsorption study of CO2 and N2 on synthesized zeolites 13X, 4A, 5A,

and beta. J Chem Eng Data 12:5648–5664. https://doi.org/10.1021/acs.jced.9b00690

Kim DJ, Kim JM, Yie JE, Seo SG, Kim SC (2004) Adsorption and conversion of various hydrocarbons on monolithic hydrocarbon adsorber. J Colloid Interface Sci 274:538–542. https://doi.org/10.1016/j.jcis.2003.12.038

Lai Z, Bonilla G, Diaz I, Nery JG (2003) Micro structural optimization of a zeolite membrane for organic vapor separation. J NCBI 300:456–460. https://doi.org/10.1126/science.1082169

Larsen SC (2007) Nanocrystalline zeolites and zeolite structures: synthesis, characterization, and applications. J Phys Chem C 111(50):18464–18474. https://doi.org/10.1021/jp074980m

Li HX, Donohue JM, Chrmier WE, Chu YF (2005) Application of zeolites as hydrocarbon traps in automotive emission controls. Stud Surf Sci Catal 158:1375–1382. https://doi.org/10.1016/S0167-2991(05)80487-2

Madasamy T, Pandiaraj M, Balamurugan M, Karnewar S, Benjamin AR, Venkatesh KA, Vairamani K, Kotamraju S, Karunakaran C (2012) Virtual electrochemical nitric oxide analyzer using copper, zinc superoxide dismutase immobilized on carbon nanotubes in polypyrrole matrix. Talanta 100:168–174. https://doi.org/10.1016/j.talanta.2012.08.033

Mani M, Subash C, Nagarajan G (2009) Performance emission and combustion characteristics of a DI diesel engine using waste plastic oil. Appl Therm Eng 29:2738–2744. https://doi.org/10.1016/j.applthermaleng.2009.01.007

Melkon Tatlier, Mesut Demir, Begum Tokay, Ayse ErdemS enatalar, Lioubov Kiwi-Minsker (2006) Substrate heating method for coating metal surfaces with high-silica zeolites: ZSM-5 coatings on stainless steel plates. J Micro Porous Mesoporous Mater 11:034. https://doi.org/10.1016/j.micromeso.2006.11.034

Miandad R, Barakat MA, Rehan M, Aburiazaiza AS, Gardy J, Nizami AS (2018) Effect of advanced catalysts on tire waste pyrolysis oil. Process Saf Environ Protect 116:542–552. https://doi.org/10.1016/j.psep.2018.03.024

Nikolajsen L, Kiwi-Minsker A, Renken (2006) Structured fixed-bed adsorber based on zeolite/sintered metal fibre for low concentration VOC removal. Chemical Engineering Research and Design 84: 562-568562 568. https://doi.org/10.1205/cherd.05220

Ojuva A, Jarvelainen M, Bauer M, Keskinen L, Valkonen M, Akhtar F, Levanen E, Bergstrom L (2015) Mechanical performance and CO2 uptake of ion-exchanged zeolite A structured by freeze-casting. J Eur Ceram Soc 35:2607–2618. https://doi.org/10.1016/j.jeurceramsoc.2015.03.001

Prasad CV, Swamy BY, Sudhakar H, Sobharani T, Sudhakar K, Subha MCS, Rao KC (2011) Preparation and characterization of 4A zeolite-filled mixed matrix membranes for pervaporation dehydration of isopropyl alcohol. J Appl Polym Sci 121:1521–1529. https://doi.org/10.1002/app.33688

Premkumar S, Balaji G (2021) Experimental investigation of HC and CO emission reduction from a diesel engine powered by plastic oil blend using fly ash as catalyst. J Therm Anal Calorim 10973:020–10541. https://doi.org/10.1007/s10973-020-10541-0

Raganati F, Ammendola P, Chirone R (2014) CO2 adsorption on fine activated carbon in a sound assisted fluidized bed: effect of sound intensity and frequency, CO2 partial pressure and fluidization velocity. Appl Energy 113:1269–1282. https://doi.org/10.1016/j.apenergy.2013.08.073

Raj BK, Jyothi Y, Kanasani P, Siva Gangadhar D (2019) the best suitable alternative to diesel in a compression ignition engine between waste plastic oil and waste tire oil blends with diesel, Energy Sources. Part a: Recovery Util Environ Effects 42:2731–2741. https://doi.org/10.1080/15567036.2019.1618985

Sachuthananthan B, Balaji G, Krupakaran RL (2019) Investigation on the use of plastic pyrolysis oil as alternate fuel in a direct injection diesel engine with titanium oxide nanoadditive. Environ Sci Pollut Res 26:10319–10332. https://doi.org/10.1007/s11356-019-04293-0

Singha, Biswajit Rujb RK, Sadhukhana AK, Guptaa P, Tiggac VP (2019) Waste plastic to pyrolytic oil and its utilization in CI engine: performance analysis and combustion characteristics. J Fuel, 28: 0016-2361. https://doi.org/10.1016/j.fuel.2019.116539

Singh RK, Ruj B (2015) Plastic waste management and disposal techniques – Indian scenario. Int J Plast Technol 19:211–216. https://doi.org/10.1007/s12588-015-9120-5

Singh RK, Ruj B, Sadhukhan AK, Gupta P (2019) Impact of fast and slow pyrolysis on the degradation of mixed plastic waste: product yield analysis and their characterization. J Energy Inst 92:1–11. https://doi.org/10.1016/j.joei.2019.01.009

Subramanian, Balaji, and Venugopal Thangavel (2020) Experimental investigations on performance, emission and combustion characteristics of diesel-hydrogen and diesel-HHO gas in a dual fuel CI engine International Journal of Hydrogen Energy 45, no. 46: 25479–25492. https://doi.org/10.1016/j.ijhydene.2020.06.280

Tang H, Li N, Li G, Aiqin Wang Yu, Cong GX, Wanga X, Zhang T (2012) Synthesis of gasoline and jet fuel range cycloalkanes and aromatics with poly (ethyleneterephthalate) wastes. Royal Soc Chem 00:1–3. https://doi.org/10.1039/C9GC00571D

Toops TJ, Nguyen Ke, Foster AL, Bunting BG, Ottinger NA, Pihl JA, Hagaman EW, Jiao J (2010) Deactivation of accelerated engine-aged and field-aged Fe–zeolite SCR catalysts. Catal Today 151:257–265. https://doi.org/10.1016/j.cattod.2010.01.019

Vijayaragavan, Mathanraj, Balaji Subramanian, Sudhakar S, and Natrayan L (2022) Effect of induction on exhaust gas recirculation and hydrogen gas in compression ignition engine with simarouba oil in dual fuel mode International Journal of Hydrogen Energy 47, no. 88: 37635–37647. https://doi.org/10.1016/j.ijhydene.2021.11.201

Xia X, Tang Y (2012) Isotope fractionation of methane during natural gas flow with coupled diffusion and adsorption/desorption. Geochim Cosmochim Acta 77:489–503. https://doi.org/10.1016/j.gca.2011.10.014

Zamani F, Rezapour M, Kianpour S (2013) Immobilization of L-lysine on zeolite 4A as an organic-inorganic composite basic catalyst for synthesis of α, β-unsaturated carbonyl compounds under mild conditions. Bull Korean Chem Soc 34:2367–2374. https://doi.org/10.5012/bkcs.2013.34.8.2367

Zhang FZ, Fuji M, Takahashi M (2005) Effect of mesoporous silica buffer layer on the orientation of MFI zeolite membranes. J Am Cermaic Soc 244:164–170. https://doi.org/10.1111/j.1551-2916.2005.00386.x

Zhang Runduo, Liu Ning, Lei Zhigang, Chen Biaohua (2016) Selective transformation of various nitrogen-containing exhaust gases toward N2 over zeolite catalysts. Chemical reviews 116:3658–3721. https://doi.org/10.1021/acs.chemrev.5b00474

Zhao Q, Qian J, An Q, Gao C, Gui Z, Jin H (2009) Synthesis and characterization of soluble chitosan/sodium carboxymethyl cellulose polyelectrolyte complexes and the pervaporation dehydration of their homogeneous membranes. J Membr Sci 333:68–78. https://doi.org/10.1016/j.memsci.2009.02.001

Publisher's note Springer Nature remains neutral with regard to jurisdictional claims in published maps and institutional affiliations.